CORA Cork Open Research Archive
Cartlann Taighde Oscailte Chorcaí

Title	Typical tropospheric aerosol backscatter profiles for Southern Ireland: The Cork Raman lidar
Authors	McAuliffe, Michael A. P.;Ruth, Albert A.
Publication date	2013-02-01
Original Citation	MCAULIFFE, M. A. P. & RUTH, A. A. 2013. Typical tropospheric aerosol backscatter profiles for Southern Ireland: The Cork Raman lidar. Atmospheric Research, 120–121, pp.334-342. http://dx.doi.org/10.1016/j.atmosres.2012.09.020
Type of publication	Article (peer-reviewed)
Link to publisher's version	10.1016/j.atmosres.2012.09.020
Rights	© 2013, Elsevier. NOTICE: this is the author's version of a work that was accepted for publication in Atmospheric Research. Changes resulting from the publishing process, such as peer review, editing, corrections, structural formatting, and other quality control mechanisms may not be reflected in this document. Changes may have been made to this work since it was submitted for publication. A definitive version was subsequently published in Atmospheric Research, [120-121, February 2013] http://dx.doi.org/10.1016/j.atmosres.2012.09.020 - https://creativecommons.org/licenses/by-nc-nd/4.0/
Download date	2026-11-16 06:31:08
Item downloaded from	https://hdl.handle.net/10468/887

UCC
University College Cork, Ireland
Coláiste na hOllscoile Corcaigh

Typical tropospheric aerosol backscatter profiles for Southern Ireland: the Cork Raman LIDAR

Michael A.P. McAuliffe and Albert A. Ruth*

Physics Department and Environmental Research Institute, University College Cork, Cork Ireland

Keywords: Vertical Aerosol Profiling, Raman Lidar, Extinction and Backscatter Coefficient, EARLINET

Abstract

A Raman lidar instrument (UCLID) was established at University College Cork and Raman backscatter coefficients, extinction coefficients and lidar ratios were measured within the period 28/08/2010 and 28/04/2011. Typical atmospheric scenarios over Southern Ireland in terms of the aerosol load in the planetary boundary layer are outlined. The lidar ratios found are typical for marine atmospheric condition (lidar ratio ca. 20-25 sr). The height of the planetary boundary layer is below 1000 m and therefore low in comparison to heights found at other lidar sites in Europe. On the 21st of April a large aerosol load was detected, which was assigned to a Saharan dust event based on HYSPLIT trajectories and DREAM forecasts along with the lidar ratio (70 sr) for the period concerned. The dust was found at two heights, pure dust at 2.5 km and dust mixing with pollution from 0.7 to 1.8 km with a lidar ratio of 40 – 50 sr.

*Corresponding author at: A. A. Ruth, Tel: +353-21-4902057, Fax: +353-21-4276949.

E-mail address: a. ruth@ucc.ie

1. Introduction

Raman lidar systems are now widely used for profiling vertical distributions of aerosol in the atmosphere (Amiridis et al., 2011; Groß et al.; Lu et al., 2011). Depending on the sophistication of the instrument the shape and microphysics of aerosol particles can be established. The eruption of Eyjafjallajökull in Spring 2010 is a very good example to illustrate the capability of Raman setups that are networked across a continent (Böckmann et al., 2004; Matthias et al., 2004a; Pappalardo et al., 2004; Sicard et al., 2012; Perrone et al., 2012). As opposed to elastic instruments, Raman lidars have the advantage that the inelastic backscatter is only affected by aerosol extinction. Since the aerosol extinction of the atmosphere is measured with the inelastic backscatter (without relying on assumptions about the aerosol type), there is no need to estimate the lidar ratio for data analysis as required by the Klett approach (Klett, 1981, 1985). This makes the Raman lidar approach superior to systems such as elastic lidars and ceilometers, where only the elastic backscatter is detected.

A Raman lidar system was recently implemented at University College Cork, Ireland. The system (named UCLID) was setup to contribute to the 'European Aerosol Research Lidar Network' (EARLINET) (Böckmann et al., 2004; Matthias et al., 2004b; Pappalardo et al., 2004) consisting of over 25 stations distributed across Europe [http://www.earlinet.org]; Being the only site in Ireland and the U.K. located in the Atlantic at the western edge of Europe (51.53N 8.29W), the Cork station is of obvious geographic importance as an entrance point of air masses into continental Europe from a north-westerly direction. The remit of the Cork station is to actively contribute to the network EARLINET and the 'Aerosols, Clouds, and Trace gases Research InfraStructure Network' (ACTRIS, http://www.actris.net) through the collection of quantitative data on the vertical aerosol profiles over Southern Ireland.

UCLID was designed for the retrieval of vertical aerosol profiles at low altitudes. The purpose of this paper is to characterize the performance of the instrument and to illustrate its specifications through measurements in clear and aerosol loaded atmosphere over Cork between 28th August 2010 and 28th of April 2011. Section 2 describes the experimental layout. Section 3 discusses the theoretical overlap compared to a experimentally determined overlap based on Wandinger and Ansmann, 2002, and the need for overlap correction is examined. In Section 4 aerosol profiles for three atmospheric scenarios are exemplified and the planetary boundary layer heights are discussed.

2. Experimental setup

Fig. 1(a) shows a schematic diagram of the transmitter, receiver and detection optics of the Raman lidar setup. The light source is a frequency doubled Nd:YAG laser (Quantel, BRILL/IR-20, 532 nm) operating at 20 Hz repetition rate with a beam diameter at the laser's exit aperture of 6 mm. The energy per pulse of ~150 mJ is measured with a power meter (PM, Gentec QE 12) before and after each measurement. The beam expander used is a refractor telescope of Galilean design, which expands the laser beam by a factor of 12. An elliptical mirror ($\lambda/8$) is used to control the overlap between the transmitter and receiver.

The receiver telescope is of Newtonian design, with a 0.3 m parabolic mirror and a focal length of 1.5 m. The field stop can be varied from 0.9 mm to 5.0 mm allowing the field of view (FOV) of the telescope to range from 0.60 mrad to 3.33 mrad, respectively. A typical field stop size would be 1.1 mm which provides a field of view of 0.73 mrad. The field stop size of 1.1 mm provides enough light suppression in the near field of the telescope but allows for a complete overlap at a low altitude. A collimating lens creates a parallel beam with a diameter of 30 mm. A 45^o beam splitter (BS1) with a reflectivity of R = 0.99 at 532.1 nm and a transmission of T = 0.97 at 607.4 nm separates the elastic backscatter from the inelastic N_2 backscatter.

The *inelastic backscatter* passes through an optional neutral density filter, whose optical density can be chosen between 0 and 5 (in steps of 0.5) to avoid saturation of the signal under different atmospheric conditions. The light is further spectrally filtered by a narrow bandwidth interference filter (IF, Barr Ltd.) at 607.40 ± 0.34 nm. Off resonance the filter suppresses stray light by more than a factor of 10^{-8} with a max transmission of 11.4% at 607 nm. Finally a positive lens (L) causes the light to converge towards the 20 mm^2 cathode of a cooled GaAsP photomultiplier (PMT, Hamamatsu H7422) with a rise time of 1 ns and a FWHM of ca. 8 ns at a gain of 2×10^6. All measurements were performed by photon counting.

The *elastic backscatter* signal can be monitored with a high resolution CMOS camera which is used to view an image of the field stop for alignment purposes. The overlap between the expanded laser beam and the telescope's FOV can be monitored using the trigger software of the camera. Approximately half of the elastic backscatter is guided through a neutral density filter and a narrow band IF filter with the centre wavelength at 532.08 ± 1.00 nm for normal incidence with a max transmission of 35.5% at 532 nm. The elastic backscatter is detected by

a bialkali PMT (Hamamatsu, H5783-P) with a cathode area of ca. 50 mm^2, a pulse rise time of 0.8 ns and FWHM of 8 ns.

Data acquisition is performed using a dual input photon counter card (Fast Comtec P7882). The bin width of the transient recorder is 200 ns, which corresponds to a minimum height resolution of 30 m. The detection optics are contained within a light tight box in line with the output from the receiver telescope. A sketch of the system showing the individual components is shown in Fig. 1(b). The laser (yellow) and beam expander (blue) are located below the detection optics together with the beam steering mirror. Power supplies and the computer controlling the data acquisition are on the same frame as the optics (Fig. 1(b)).

The analysis procedures (Pappalardo et al., 2004) for the inversion algorithms for both elastic and Raman lidar data has been quality assured within EARLINET using the same data and comparison as outlined in Böckmann et al., 2004.

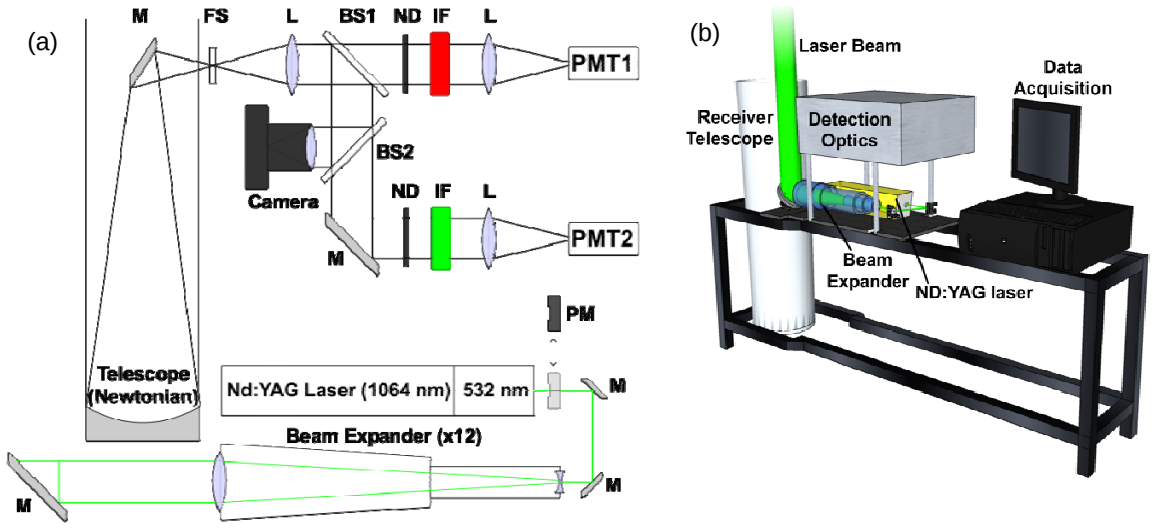


Fig. 1. (a) Schematic of the Rama lidar system UCLID: PM: power meter (optional) FS: Field stop (diameter 0.9 – 5 mm, corresponding FOV 0.6 – 3.33 mrad). L: Lens collimates the beam onto a wavelength dependent beam splitter, BS1. Dichroic beam splitter, BS2: Beam splitter (50:50 ratio). Camera: CMOS is used to monitor the fieldstop. ND: neutral density filters (optional), IF: Interference filter (narrow band), PMT: photomultiplier tube (1:cooled GaAsP, 2:uncooled bialkali). **(b)** UCLID setup, computer (data acquisition), beam expander and Nd:YAG laser, detection optics aligned with the output of the receiver telescope.

3. Overlap function

The overlap between the laser beam and the telescope's field of view (FOV) as a function of altitude, *z*, is described by the overlap function, *O*(z). *O*(z) is critically dependent on the alignment of the laser beam with respect to the *FOV* of the telescope. With a ray tracing programme (Cash, 1994) overlap functions were simulated for the instrument's geometry and optical parameters, i.e. the primary mirror's focal length and diameter, the field stop diameter, and the distance of the beam steering mirror from the main telescope's optical axis. Based on the assumption that the overlap function for the elastic and inelastic backscatter measurement are identical, *O*(z) can be determined using the iterative approach outlined in Wandinger and Ansmann (Wandinger and Ansmann, 2002). The range-corrected ($\times z^2$) *and* overlap-corrected ($\times O(z)^{-1}$) experimental signal, $P_0(z)$, is proportional to the total backscatter coefficient, i.e. the sum of the elastic molecular backscatter coefficient at 532 nm, $\beta_{0,M}(z)$, and the Raman backscatter coefficient, $\beta_{Raman}(z)$:

$$P_0(z)O(z)^{-1}z^2 \propto \beta_{\mathrm{Raman}}(z) + \beta_{0,\mathrm{M}}(z) \tag{1}$$

The *only* range-corrected aerosol signal, is primarily a function of the total backscattering and the range-dependent overlap, as expressed by the Klett solution ($\beta_{\mathrm{Klett}}(z)$):

$$P_0(z)z^2 \propto \beta_{\mathrm{Klett}}(z) + \beta_{0,\mathrm{M}}(z) \tag{2}$$

The relative difference between the Klett and the Raman lidar solution,

$$\frac{P_0(z)O(z)^{-1}z^2 - P_0(z)z^2}{P_0(z)O(z)^{-1}z^2} \propto 1 - O(z) \tag{3}$$

can be used to calculate the overlap effect on the aerosol signal, by iteratively re-applying the Klett method to the (initially uncorrected, i = 1) elastic backscatter signal according to eq. (4), see Wandinger and Ansmann, 2002:

$$P_{0,\mathrm{i}+1}(z) = P_{0,\mathrm{i}}(z)\left[1 + \frac{\beta_{\mathrm{Raman}}(z) - \beta_{\mathrm{Klett,i}}(z)}{\beta_{\mathrm{Raman}}(z) + \beta_{0,\mathrm{M}}(z)}\right] \tag{4}$$

Typically less than 15 iterations will remove the overlap effect completely. To determine the experimental overlap profile (shown in Fig. 2), a comparison is made with the measured signal profile and the corrected signal profile.

The overlap was also simulated as a function of the angle between the symmetry axis of the telescope's field of view, *FOV*, and the laser beam direction. The angle is determined by (*FOV* / 2) – (*x* × *DIV*), where *DIV* represents the divergence of the laser beam after expansion, and *x* is a multiplier. Changing *x* allows the introduction of small changes in the angle between the laser beam axis and the telescope's *FOV* axis. For the two simulations shown in Fig. 2 the values for *x* were chosen to be 1 and 1.5 as these multipliers appeared appropriate for a comparison with the experimentally determined overlap function.

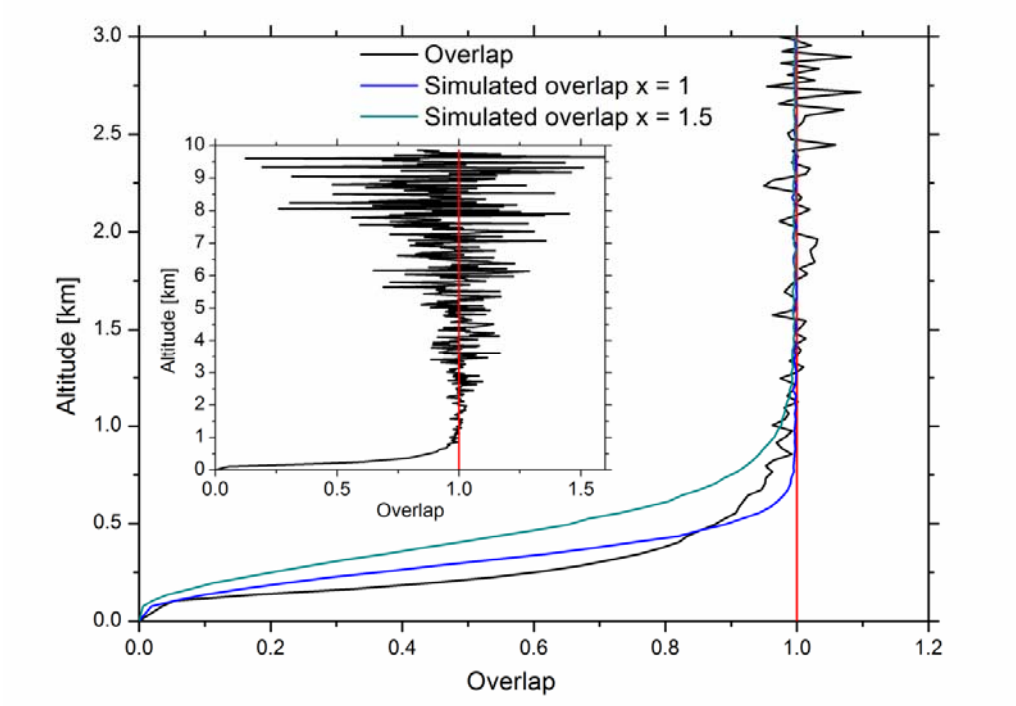


Fig. 2. Measured (black line) and calculated (blue and green line for angle difference of *x* =1 and *x* = 1.5 respectively) overlap function for UCLID. The vertical red line indicates the complete overlap, i.e. *O*(z)=1. Insert: The measured overlap function up to an altitude of 10 km.

The measured overlap of laser and *FOV* is complete at approximately 1000 m. Having a low complete overlap makes UCLID ideal for monitoring the height of the boundary layer. Based on the comparison in Fig. 2, the angle between the laser beam axis and the telescope's *FOV* axis is smaller than (0.5 × *DIV*). The accuracy for measuring the field stop diameter of UCLID is ≈0.25 mm. For the given setup, changing the field stop from 1.1 mm to 1.2 mm increases the *FOV* from 0.73 mrad to 0.80 mrad. The *FOV* for the experimentally measured overlap is possibly larger than the value used in the simulation. Therefore it is be possible to reduce the height at which the overlap is complete. If the diameter of the field stop is

unintentionally larger than required, the PMTs may be exposed to excess light in the near field of the telescope (below 700 m) causing the PMTs to saturate. This scenario has not been observed with UCLID due to carefully neutral density filter selection.

4. Results and Discussion

An upper cut off level for the uncertainty of the backscatter coefficient of 50 % has been applied to the data, therefore errors above this threshold are not considered. The same applies to the extinction coefficient and lidar ratio profiles. For the analysis of the Raman signal radiosonde data on pressure and temperature were taken from the Met Éireann station at Valentia Observatory (4 launches per day up to 2012) approximately 120 km away from the Cork site.

Fig. 3 shows a UCLID measurement on the 17th of January 2011. In Fig. 3 three profiles are compared; Two elastic backscatter profiles (referred to as 'Klett') with (blue line) and without (black line) overlap correction applied, and a Raman backscatter profile (red line). These profiles are based on the average of data taken over a 2 hr period with very clear conditions. A lidar ratio of 25 sr was used for the calculation of the Klett solutions.

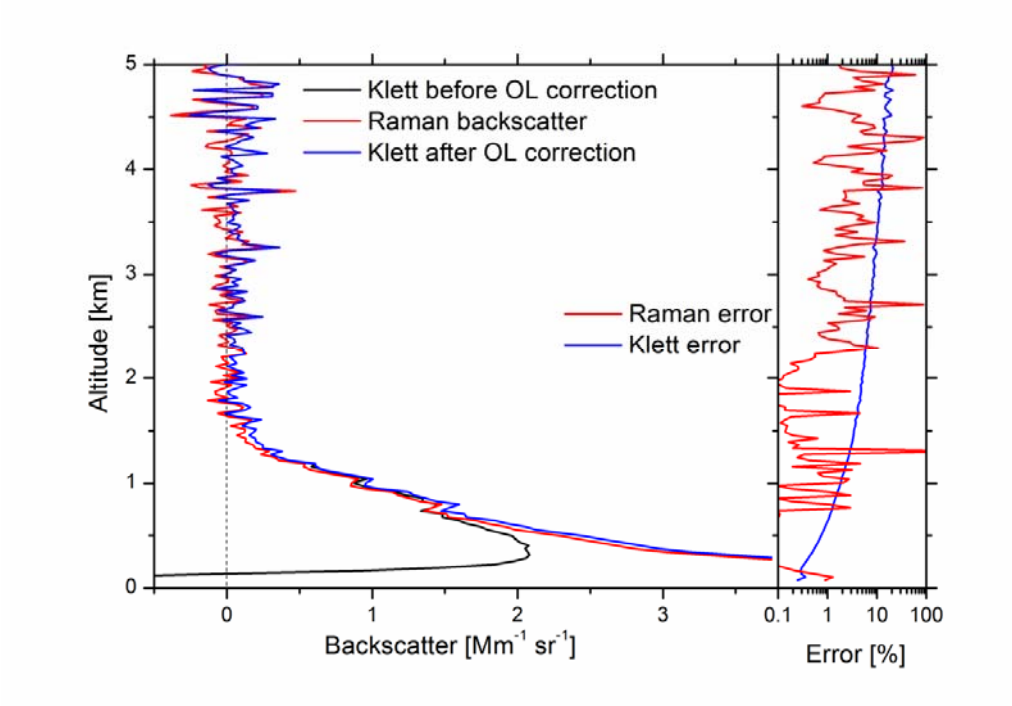


Fig. 3. Left: Comparison between an overlap corrected (blue line) and uncorrected (black line) elastic backscatter profile (Klett) and a Raman backscatter profile (red line). Right: Percentage error for the Klett (blue line) and Raman (red line) backscatter solutions. (OL = overlap)

Since the Raman backscatter profile is independent of the overlap function, it can be directly compared with the corrected Klett solution (Fig. 3), and the agreement is satisfactory. At altitudes larger than approximately 700 m all three profiles (including the uncorrected Klett solution) agree very well. Below that altitude, however, the uncorrected Klett solution strongly deviates from the other two profiles, illustrating the necessity to perform an overlap correction. The percentage errors of the Raman backscatter (red) and Klett solution (blue) are shown in the right panel of Fig. 3. The latter gradually reaches 20% at 5 km. The substantial variation in the error of the Raman backscatter is due the inelastic signal being significantly weaker.

Fig. 4 shows (a) the backscatter coefficient (b) the extinction coefficient and (c) the lidar ratio for a measurement on the 6th of January 2011, determined using the Raman method. The extinction coefficient has an overlap correction applied with smoothing window lengths of 750 m from altitudes of 270 m to 2370 m, and of 870 m from 2370 m upwards. The lidar ratio has a smoothing window length of 900 m. The profile was measured with an integration time of 1 hr. The signal has been corrected for overlap using the OL function in Fig. 2. Errors shown have been calculated from the standard deviation caused by signal noise. The lidar ratio has only been evaluated up to 2 km due to the strongly increasing uncertainty of the weak inelastic signal with increasing altitude. The lidar ratio is characteristic for marine conditions in the planetary boundary layer, a typical scenario for the Cork site (Weitkamp, 2005). Based on the backscatter signal, panel (a) shows the presence of a cirrus cloud between 5.5 km and 7 km, which is in the typical altitude range of 5-12 km for cirrus clouds in Ireland (Verrabuthiran, 2004). No other information about the cirrus cloud can be derived as the extinction coefficient becomes unreliable above 2 km. Typical extinction coefficients at the planetary boundary layer are in agreement with values reported for Aberystwyth (see Fig. 6 in Matthias et al., 2004 in comparison to Figs. 4b, 5b and 7b), which has the most comparable climatic condition within the EARLINET network. The Cork extinction values are somewhat smaller (mean aerosol optical depth within the planetary boundary layer (PBL) was 0.048 with standard deviation of 0.031 for 532nm;[1] compare with Fig. 2b in Wandinger et al., 2004) which can be expected since the Wales lidar operated at 355 nm.

[1] The aerosol optical depth was calculated by integration from the top of the PBL to the ground using a constant value of the lowest experimentally available data point down to ground level (for that a constant aerosol extinction coefficient in this lowest range above ground was assumed).

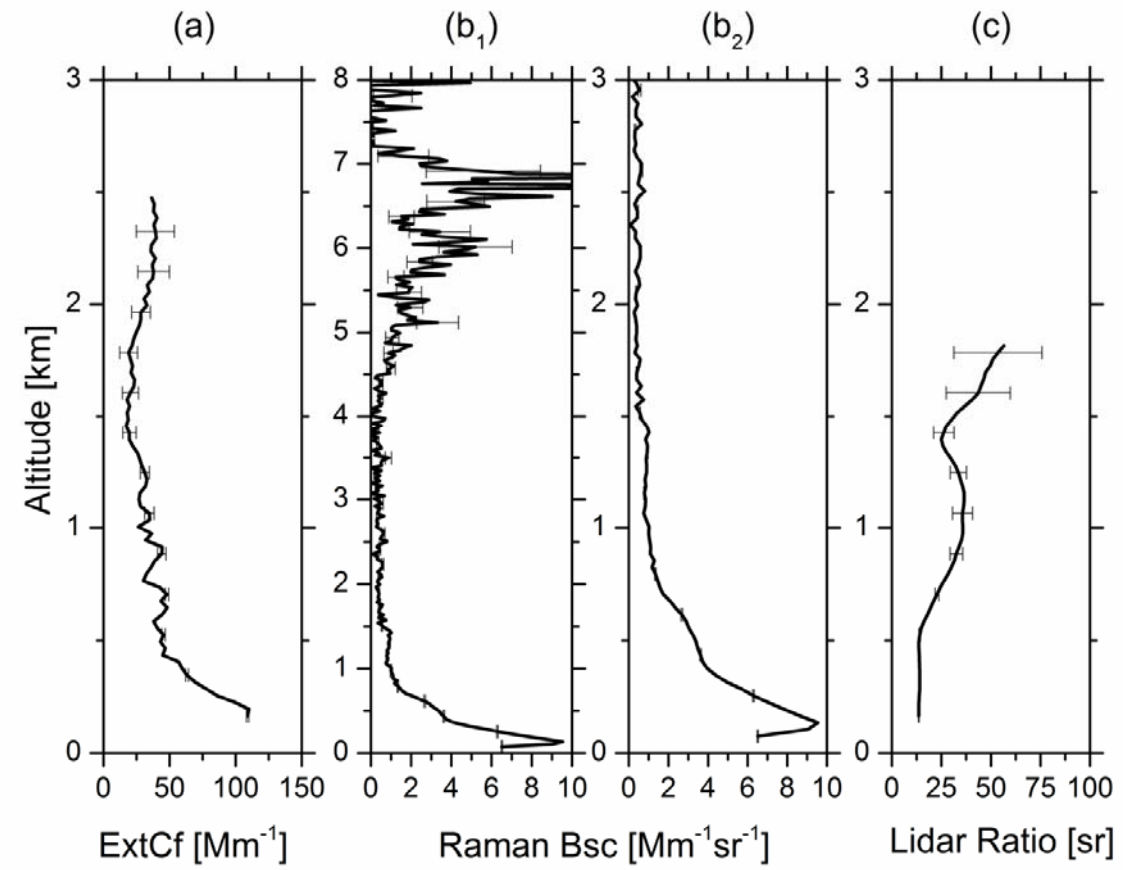


Fig. 4. Measurement on the 6th of January 2011 (1800-1900 hrs). (a) Extinction coefficient (ExtCf) with errors (signal smoothing with window lengths of 750 m between 270 m and 2370 m and 870 m from 2370 m upwards, (b_1) Raman backscatter (Bsc) solution with errors (up to 8 km); cirrus cloud between 5.5 and 7 km. (b_2) Data from panel (b_1) for altitudes up to 3 km. (c) Lidar ratio with a smoothing window of 630 m. Error bars indicate the standard deviation caused by signal noise.

Fig. 5 show an example of an aerosol event detected at the Cork site on 21 April 2011. Panels (a), (b), and (c) show the backscatter coefficient, the extinction coefficient and the lidar ratio as a function of altitude, respectively. The integration time was 30 minutes. The top of the planetary boundary layer was determined to be 615 ± 30 m. This height was calculated using the 1st derivative of the backscatter coefficient as described in (Bösenberg and Matthias, 2003). The top of the PBL is defined as the steepest gradient of the profile of the particle backscatter signal, i.e., the largest local minimum of the first derivative of the range-corrected signal. In the left panel of Fig. 6, a backward trajectory (4 days) is shown as determined by the HYSPLIT (HYbrid Single-Particle Lagrangian Integrated Trajectory) model (Draxler and Hess, 1997) using GDAS (Global Data Assimilation System - http://ready.arl.noaa.gov/gdas1.php) meteorological data. The model implies that the air

masses over Cork on that day arrived from in Western Europe, indicating that the measured layer may be due to continental aerosol. The Dust Regional Atmospheric Model (DREAM) (Nickovic et al., 2001) is capable of predicting major dust events. Using the forecasts available at http://www.bsc.es/projects/earthscience/DREAM, a large dust event was forecasted for the end of April 2011. According to the model on the 21st of April dust was present over Spain and southern France; these locations match with the blue, cyan and green traces on the HYSPLIT backward trajectory (see Fig. 6, left panel). From the Raman backscatter profile (Fig. 5(a)) a large aerosol layer was detected between 0.7 and 2 km and another at 2.5 km, these correlate to the green, blue (0.7 – 2 km) and cyan (2.5 km) traces on the HYSPLIT model (left panel, Fig. 6). While the backward trajectory (red line, Fig.6 left panel) suggests that the layer between 500 m to 800 m passed over Western Europe, it is likely that mixing with local marine aerosol from the Celtic Sea is taking place during the transport to Cork. Given the low top altitude of the PBL and the strong marine layer above the PBL it can be concluded that the layer at 2.5 km is a pure dust layer with a lidar ratio of 70 sr, while the layer from 1.0 to 1.8 km contains dust, marine and anthropogenic particles (lidar ratio 40 to 50 sr). The lidar ratios agree well with the ones measured in (Papayannis et al., 2008). While DREAM forecast the dust entering Ireland's atmosphere on the 23rd of April, the event was measured 30 hr before the model prediction. This is again illustrated in the left panel of Fig. 6, where the data from DREAM are overlayed with trajectories from HYSPILT. The figure also shows the prevailing wind directions at the time relevant for Ireland. The right panel of Fig. 6 shows the colour-coded image of the range corrected 532 nm backscatter signal vs. time where the layer between 0.7 km and 2.0 km is clearly evident. Another aerosol layer starts to become evident at ca. 2.5 km altitude approximately at 2155 hrs (Fig. 6).

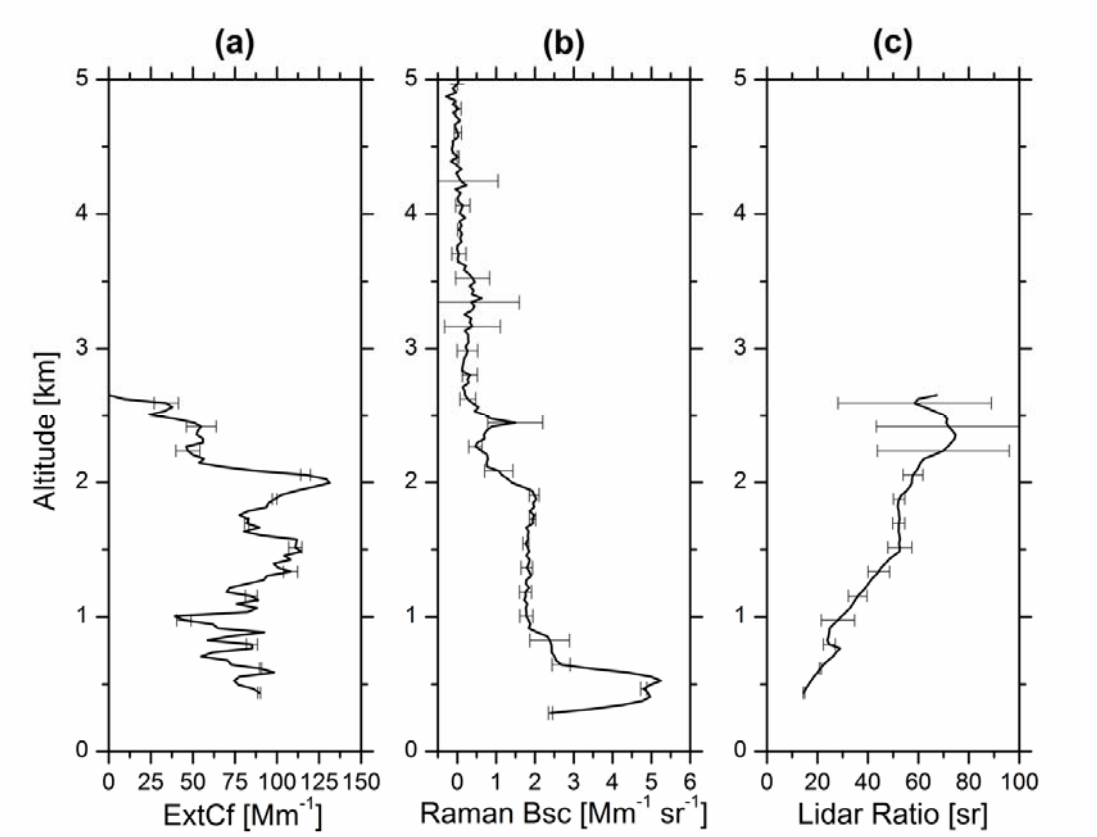


Fig. 5. Measurement on the 21st of April 2011 (2130-2200 hrs). (a) Extinction coefficient (ExtCf) with errors (signal smoothing with window lengths of 250 m up to 960 m, 390 m between 960 and 2490 m, and 570 m from 2490 m upwards. (b) Raman backscatter (Bsc) solution with errors (up to 5 km). (c) Lidar ratio with a smoothing window of 270 m. An aerosol layer is evident between 0.5 – 2 km with a lidar ratio between 20 and 60 sr. Error bars indicate the standard deviation caused by signal noise.

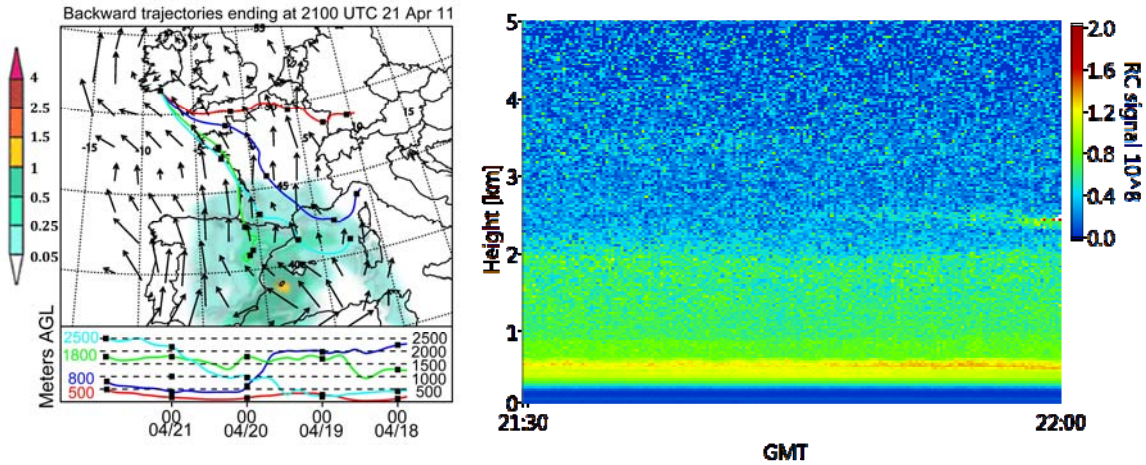


Fig. 6. Left: NOAA HYSPLIT model backward trajectories for four days before 21st of April. The map includes the colour-coded (unit: g/m^2) image is from the DREAM forecast for the 21st of April, 1200 hrs. Wind directions are also indicated. A dust event was predicted over Spain and southern France as indicated by the image. Trajectories indicate aerosols arrived at Cork from the European continent. Right: Colour-coded image of time-dependent range corrected 532 nm backscatter profiles of the measurement on the 21st of April for a 30 min period. A wide aerosol layer is evident between 0.5 km and 2.0 km.

The panels (a_1) and (a_2) in Fig. 7 show the Raman backscatter coefficient, panel (b) the extinction coefficient, and (c) the lidar ratio for the 28th of April 2011. In panel (a_1) the detection of a cirrus cloud at the upper end of the typical range between 11 and 12 km is evident; panel (a_2) is an enlargement of (a_1) plotted to an altitude of 5 km to provide more detail of the lower atmosphere. The lidar ratio is only plotted up to 1.5 km due to the large uncertainty in the inelastic signal. The corresponding Fig. 8 (left panel) shows a backward trajectory (4 days) and a colour-coded image of time-dependent range corrected 532 nm backscatter profiles (right panel). According to the HYSPLIT model the air masses probed on 28 April had passed over Scotland and the English West coast (blue and red trace). The right panel in Fig. 8 illustrates the layer between 1.0 and 1.5 km. The extinction coefficient is valid up to approximately 2.5 km, due to a small signal-to-noise ratio. The height of the PBL was determined to be rather low at 705 ± 30 m with a lidar ratio at that altitude of 35 ± 6 sr. The layer between 1.0 and 1.5 km has a lidar ratio of 48 ± 4 sr. These ratios suggest anthropogenic particles from the local area with additional aerosol loads arriving at Cork from central Britain according to HYSPLIT data. The observed extinction coefficients were generally consistent with published values in clean maritime environments (Ackermann, 1998; Masonis et al., 2003).

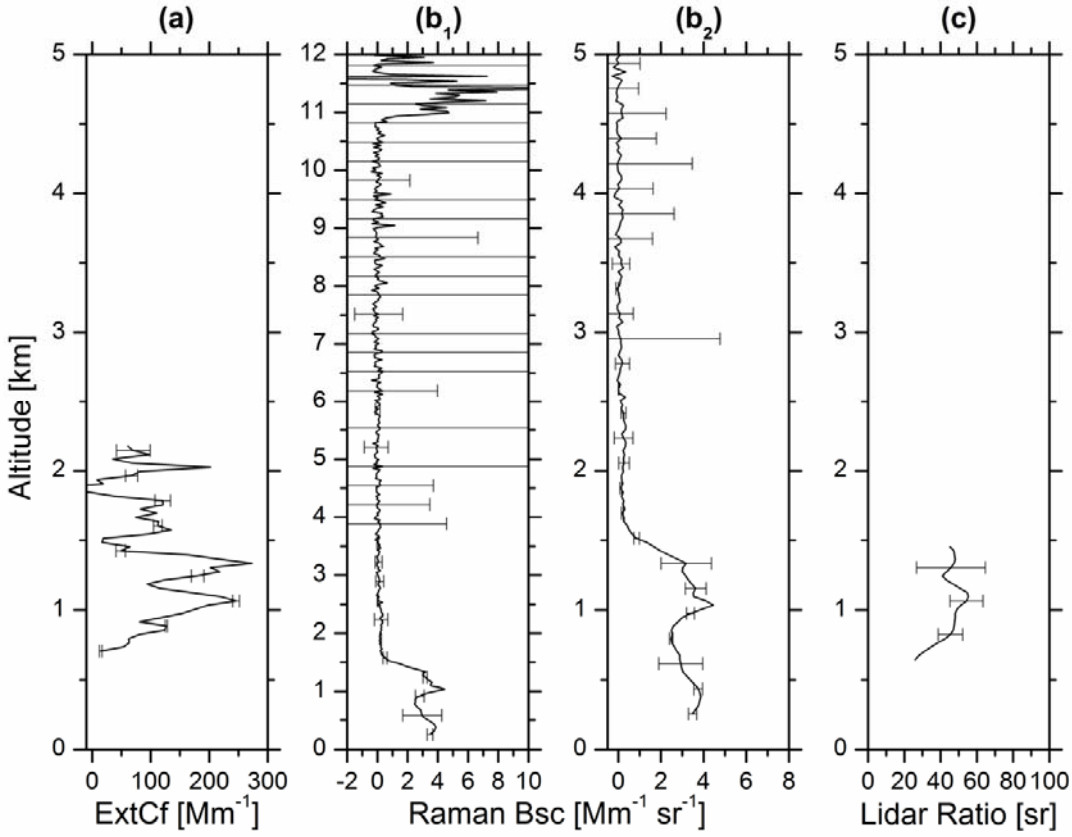


Fig. 7. Measurement on the 28th of April 2011 (2130-2200 hrs). (a) Extinction coefficient (ExtCf) with errors (signal smoothing with window lengths of 90 m up to 450 m, of 450m between 450 and 1980 m, and 780 m from 1980 m upwards. (b_1 and b_2) Raman backscatter (Bsc) solution with errors (up to 12 and 5 km, respectively). (c) Lidar ratio with a smoothing window of 120 m. Cirrus cloud is apparent in panel (a_1) at 11-12 km. An aerosol layer is evident between 1 and 1.5 km with a lidar ratio between 45 and 60 sr. Error bars indicate the standard deviation caused by signal noise.

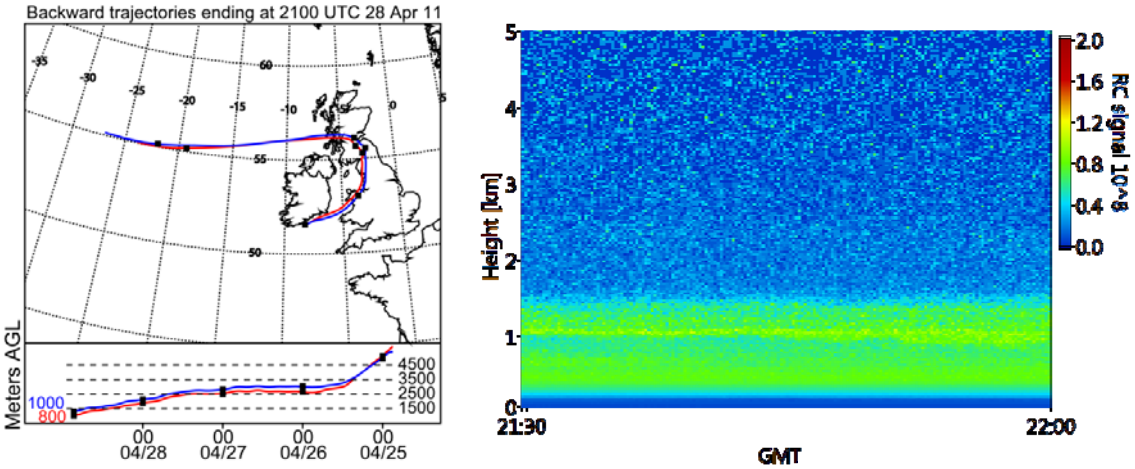


Fig. 8. Left: NOAA HYSPLIT model backward trajectories for five days before 28th of April. Trajectories indicate aerosols arrived at Cork from Scotland and the English West coast. Right: Colour-coded image of time-dependent range corrected 532 nm backscatter profiles of the measurement on the 28th of April for a 30 min period. An aerosol layer is evident between 1.0 km and 1.5 km.

Fig. 9 shows a summary of a selection of measurements for the period from the 28th of August 2010 to the 28th of March 2011 concerning the height of the PBL and the lidar ratio at that height. The lidar ratio of the PBL was determined by taking the mean of all ratios within the PBL, the error is due to the standard deviation within the PBL. The height of the PBL was typically established after dusk, using 1 to 1.5 hr integration times with the exception of the measurements on the 18th and 22nd of November 2010 (the latter measurements were taken 1-2 hr before sunset in the afternoon between 15:00 to 16:00 hrs where it was impossible to measure extinction coefficients due to a strong stray light background). The average of the top of the PBL was found to be very low at ca. 685 ± 70 m based on the Raman lidar measurements shown in Fig. 9 (excluding the data points in November 2010, since they were taken during daytime). Even though the number of measurements presented is statistically not significant (and the error has already been weighted accordingly) this appears significantly lower than for other European lidar stations (Matthias et al., 2004a), especially in comparison with Aberystwyth where a PBL height of ca. 1200 ± 480 m was reported over a two year period (55 measurements were taken into account). Just like in Cork there was also no notable trend of the PBL height concerning seasons in Wales (Matthias2004a). The generally lower average temperature in Cork in connection with small seasonal changes may be reason for the seemingly lower PBL height. However, more UCLID data are required to confirm this. The typical lidar ratios within the PBL found at the Cork site are between 20 and 40 sr and illustrate that the aerosol loading of the troposphere over Cork is governed by marine influences due to the proximity of the site to the Celtic Sea.

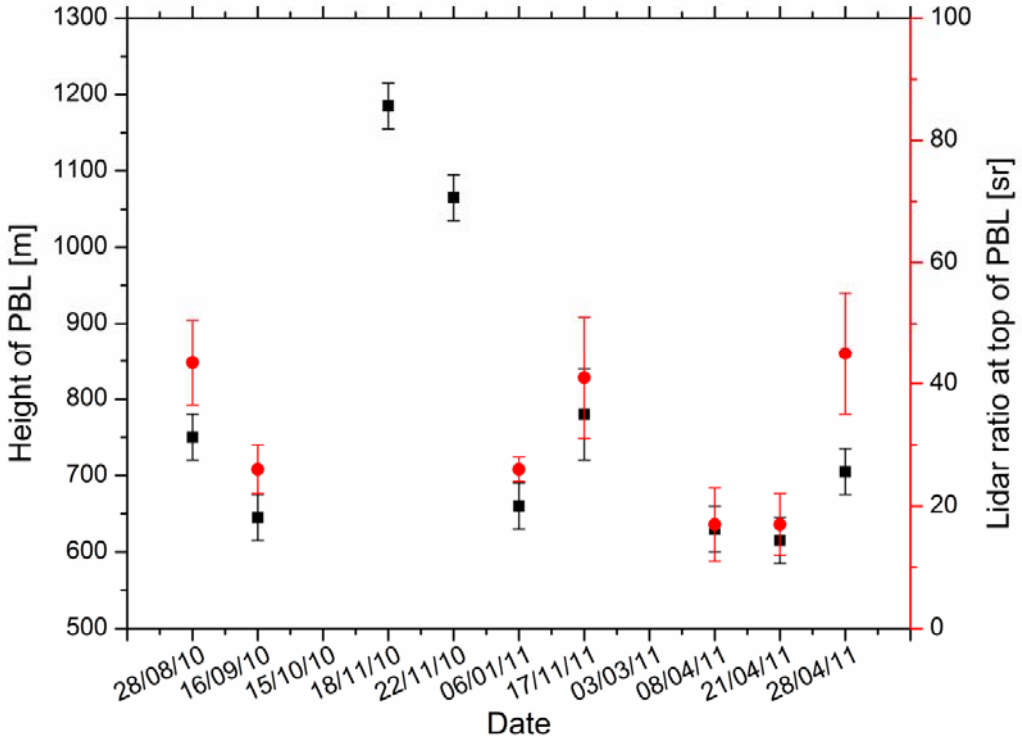


Fig. 9. Measured heights of planetary boundary layer (black squares) shown with corresponding lidar ratio at the PBL height (red dots).

General conditions for backscatter lidar research at Cork and summarizing remarks

The location of the Cork lidar is of noteworthy benefit to the EARLINET and ACTRIS networks concerning its geographic location in the north-west of Europe. Typical aerosol scenarios are largely influenced by air masses from North America, Northern Europe and depending on transport conditions also North Africa and Western Europe. It is worth noting that Ireland is also a potential entry point for air-masses from Iceland in case of volcanic activity as encountered in 2010. However, weather conditions in Cork can be adverse when it comes to a high frequency of lidar operation. Generally, the climate in Cork is mild but changeable with a lot of rainfall and a lack of temperature extremes. Cork Airport records an average of 1194.4 millimetres of precipitation annually. There are on average 151 days a year with more than 1 mm of rainfall, of which there are 75 days with rain over 5 mm. Cork is generally foggy, with an average of 100 days of fog per year, typically occurring in the morning and winter. The yearly average of sunshine is 3.8 hr per day, with 69 days where no sunshine was recorded. The yearly average wind speed is 33 kph, while the most frequent wind directions are West, West South West, South South West and North North West (see

Fig. 10, which shows the wind direction and frequency of wind speeds in the Cork region from August 2010 to April 2011). The mean relative humidity for an average year is recorded as 85 % and on a monthly basis it ranges from 78 % in May to 90 % in October and November.

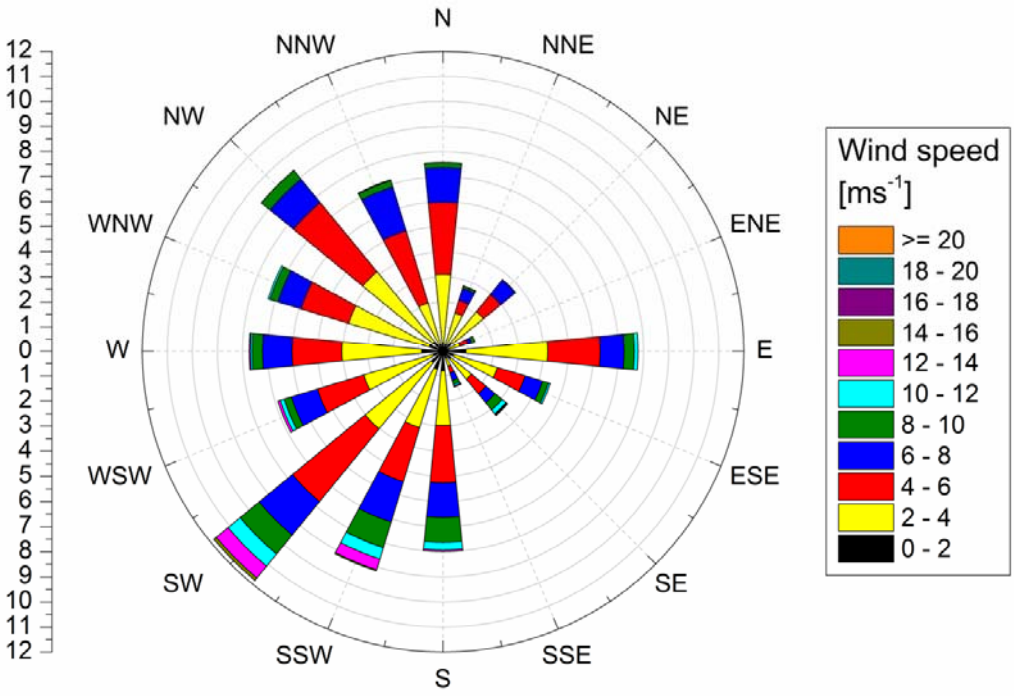


Fig. 10. Summary of wind direction and frequency of wind speeds from 1 August 2010 to 30 April 2011 for the Cork region. Axis on the left represents the percentage of wind speed that occurred in a certain direction, e.g. ca. 12% of all wind directions are from the South West in said period. The colour plot on the right represents the wind speed, e.g. for the SW direction ca. 3% of the wind had a speed between 2-4 ms^{-1} (yellow), ca. 4% between 4-6 ms^{-1} (red), ca. 2% between 6-8 ms^{-1} (blue) and so forth.

Relevant for a lidar station is the level of cloud cover (Moriarty, 1991). Table 1 and 2 show the number of days categorised by different cloud cover levels over Cork airport from the 28th of August 2010 to the 28th of April 2011. The cloud level is determined from 1 hr before sunset to 2–3 hr after sunset. These are the required times for Raman measurements set by EARLINET. Table 1 shows a full summary of 244 days between the 28th of August 2010 to the 28th of April 2011, while table 2 shows a summary of cloud conditions on the required climatological measurement days (Monday and Thursday) set by EARLINET. For climatological measurements the typical averaging time is 30 minutes, if cloud is present during a measurement, it can be removed during analysis, up to a maximum of 50%. Based

on the typical cloud cover from Table 1 67% of potentially scheduled EARLINET measurements are affected by more than 50% cloud cover.[2]

Table 1
Number of days categorised by different cloud cover over Cork airport from the 28th of August 2010 to 28th of April 2011, total number of days 244.

Cloud cover (oktas)	0	1	2	3	4	5	6	7	8
Number of days	0	30	22	16	26	20	26	50	54

Table 2
Monday and Thursday climatological sunset measurements required by EARLINET categorised by different cloud cover over Cork airport from the 28 August 2010 to 28 April 2011, total number of days 70.

Cloud cover (oktas)	0	1	2	3	4	5	6	7	8
Number of days	0	10	1	5	7	6	5	18	18

Acknowledgement

Support from Science Foundation Ireland (RFP/06/EEB011) and the Irish Research Council for Science, Engineering & Technology (EMBARK postgraduate fellowships, 2009) is gratefully acknowledged. We are also very grateful to many of the research staff at Leibniz Institute for Tropospheric Research (IfT) Leipzig (Germany) for their help and many clarifying discussions, notably Ronny Engelmann and Ina Mattis (now at Deutscher Wetterdienst Hohenpeißenberg, Meteorological Observatory, Germany) as well as Ulla Wandinger. We also thank Christie Roche, Joe Sheehan and John Lucy for their excellent technical support in setting up the new facility for the UCLID instrument.

[2] 0 oktas = clear sky, 4 oktas = sky half covered in cloud, 8 oktas = completely overcast

References

Ackermann, J., 1998. The extinction-to-backscatter ratio of tropospheric aerosol: A numerical study. J. Atmos. Ocean. Techn. 15, 1043–1050.

Amiridis, V., Balis, D., Giannakaki, E., Kazadzis, S., Arola, A., Gerasopoulos, E., 2011. Characterization of the aerosol type using simultaneous measurements of the lidar ratio and estimations of the single scattering albedo. Atmos. Res. 101, 46–53.

Böckmann, C., Wandinger, U., Ansmann, A., Bösenberg, J., Amiridis, V., Boselli, A., Delaval, A., De Tomasi, F., Frioud, M., Grigorov, I.V., Hågård, A., Horvat, M., Iarlori, M., Komguem, L., Kreipl, S., Larchevêque, G., Matthias, V., Papayannis, A., Pappalardo, G., Rocadenbosch, F., Rodrigues, J.A., Schneider, J., Shcherbakov, V., Wiegner, M., 2004. Aerosol lidar intercomparison in the framework of the EARLINET project. 2. Aerosol backscatter algorithms. Appl. Opt. 43, 977–989.

Bösenberg, J., Matthias, V., 2003. EARLINET: A European aerosol research lidar network to establish an aerosol climatology. Report: Max-Planck-Institut für Meteorologie, Hamburg, 348.

Cash, W.C., 1994. IRT ver 5.2.1 (interactive ray trace). Opensource, Colorado, Raytracing program.

Draxler, R.R., Hess, G.D.,1997. Description of the HYSPLIT_4 modeling system., NOAA Tech. Memo. ERL ARL-224, NOAA Air Resources Laboratory, Silver Spring, MD, USA, 1–24.

Groß, S., Freudenthaler, V., Wiegner, M., Gasteiger, J., Geiß, A., Schnell, F., 2012. Dual-wavelength linear depolarization ratio of volcanic aerosols: lidar measurements of the Eyjafjallajökull plume over Maisach, Germany. Atmos. Env. in press.

Klett, J.D., 1981. Stable analytical inversion solution for processing lidar returns. Appl. Opt. 20, 211–220.

Klett, J.D., 1985. Lidar inversion with variable backscatter/extinction ratios. Appl. Opt. 24, 1638–1643.

Lu, X., Jiang, Y., Zhang, X., Wang, X., Nasti, L., Spinelli, N., 2011. Retrieval of aerosol extinction-to-backscatter ratios by combining ground-based and space-borne lidar elastic scattering measurements. Opt. Express 19, A72–A79.

Masonis, S.J., Anderson, T.L., Covert, D.S., Kapustin, V., Clarke, A.D., Howell, S., Moore, K., 2003. A study of the extinction-to-backscatter ratio of marine aerosol during the shoreline environment aerosol study. J. Atmos. Ocean. Techn. 20, 1388–1402.

Matthias, V., Balis, D., Bösenberg, J., Eixmann, R., Iarlori, M., Komguem, L., Mattis, I., Papayannis, A., Pappalardo, G., Perrone, M.R., Wang, X., 2004a. The vertical aerosol distribution over Europe: statistical analysis of Raman lidar data from 10 EARLINET station. J. Geophys. Res. 109,D18201, doi:10.1029/2004JD004638.

Matthias, V., Freudenthaler, V., Amodeo, A., Balin, I., Balis, D., Bösenberg, J., Chaikovsky, A., Chourdakis, G., Comeron, A., Delaval, A., De Tomasi, F., Eixmann, R., Hågård, A., Komguem, L., Kreipl, S., Matthey, R., Rizi, V., Rodrigues, J.A., Wandinger, U., Wang, X., 2004b. Aerosol lidar intercomparison in the framework of the EARLINET project. 1. Instruments. Appl. Opt. 43, 961–976.

Moriarty, W. W., 1991. Cloud cover as derived from surface observations, sunshine duration, and satellite-observations. Solar Energy 47, 219–222.

Nickovic, S., Kallos, G., Papadopoulos, A., Kakaliagou, O., 2001. A model for prediction of desert dust cycle in the atmosphere. J. Geophys. Res. 106, 18113–18129.

Papayannis, A., Amiridis, V., Mona, L., Tsaknakis, G., Balis, D., Bösenberg, J., Chaikovski, A., De Tomasi, F., Grigorov, I., Mattis, I., Mitev, V., Müller, D., Nickovic, S., Pérez, C., Pietruczuk, A., Pisani, G., Ravetta, F., Rizi, V., Sicard, M., Trickl, T., Wiegner,

M., Gerding, M., Mamouri, R.E., D'Amico, G., Pappalardo, G., 2008. Systematic lidar observations of Saharan dust over Europe in the frame of EARLINET (2000–2002). J. Geophys. Res. 113, D10204, doi:10.1029/2007jd009028.

Pappalardo, G., Amodeo, A., Pandolfi, M., Wandinger, U., Ansmann, A., Bösenberg, J., Matthias, V., Amiridis, V., De Tomasi, F., Frioud, M., Iarlori, M., Komguem, L., Papayannis, A., Rocadenbosch, F., Wang, X., 2004. Aerosol lidar intercomparison in the framework of the EARLINET project. 3. Raman lidar algorithm for aerosol extinction, backscatter, and lidar ratio. Appl. Opt. 43, 5370–5385.

Pappalardo, G., Mona, L., Adam, M., Apituley, A., Arboledas, L.A., Chaikovsky, A., Cuesta, J., de Tomasi, F., D'Amico, G., Giannakaki, E., Grigorov, I., Gross, S., Iarlori, M., Mamouri, R.E., Mattis, I., Mitev, V., Nicolae, D., Pietruczuk, A., Serikov, I., Sicard, M., Simenov, V., Spinelli, N., Trickl, T., Wagner, F., 2012. 4D distribution of the 2010 Eyjafjallajökull volcanic cloud over Europe observed by EARLINET. Atmos. Chem. Phys. to be submitted.

Perrone, M. R., De Tomasi, F., Stohl, A. Kristiansen N. I., 2012. Characterization of Eyjafjallajökull volcanic aerosols over south eastern Italy, Atmos. Chem. Phys. Discuss., 12, 15301–15335.

Sicard, M., Guerrero-Rascado, J. L., Navas-Guzmán, F. Preißler, J., Molero, F., Tomás, S., Bravo-Aranda, J. A., Comerón, A., Rocadenbosch, F., Wagner, F., Pujadas, M., Alados-Arboledas, L., 2012. Monitoring of the Eyjafjallajökull volcanic aerosol plume over the Iberian Peninsula by means of four EARLINET lidar stations", Atmos. Chem. Phys., 12, 3115-3130.Verrabuthiran, S., 2004 High-altitude cirrus clouds and climate, Resonance 9, 23-32.

Wandinger, U., Ansmann, A., 2002. Experimental determination of the lidar overlap profile with Raman lidar. Appl. Opt. 41, 511–514.

Wandinger, U., Mattis, I., Tesche, M., Ansmann, A., Bösenberg, J., Chaikovski, A., Freudenthaler, V., Komguem, L., Linné, H., Matthias, V., Pelon, J., Sauvage, L., Sobolewski, P., Vaughan, G., Wiegner, M., 2004. Air mass modification over Europe: EARLINET aerosol observations from Wales to Belarus. J. Geophys. Res. 109, D24205, doi: 10.1029/2004jd005142.

Weitkamp, C., 2005 *Lidar: Range-resolved Optical Remote Sensing Of The Atmosphere*. Springer Science+Business Media, p 112. ISBN: 9780387400754